

SECURITY CLASSIFICATION OF THIS PAGE (When Data Entered)

REPORT DOCUMENTATION PAGE		READ INSTRUCTIONS BEFORE COMPLETING FORM	
1. REPORT NUMBER #63	PRINCETON UNIVERSITY	2. GOVT ACCESSION NO.	3. RECIPIENT'S CATALOG NUMBER
4. TITLE (and Subtitle) MOVING NONLOCAL CRACK: ANTI-PLANE SHEAR CASE		5. TYPE OF REPORT & PERIOD COVERED Technical Report	
		6. PERFORMING ORG. REPORT NUMBER 84-SM-13	
7. AUTHOR(s) N. Ari and A.C. Eringen		8. CONTRACT OR GRANT NUMBER(s) N00014-83-K-0126 Mod 4	
9. PERFORMING ORGANIZATION NAME AND ADDRESS PRINCETON UNIVERSITY Princeton, NJ 08544		10. PROGRAM ELEMENT, PROJECT, TASK AREA & WORK UNIT NUMBERS NR 064-410	
11. CONTROLLING OFFICE NAME AND ADDRESS OFFICE OF NAVAL RESEARCH (Code 471) Arlington, VA 22217		12. REPORT DATE December 1984	
		13. NUMBER OF PAGES 16	
14. MONITORING AGENCY NAME & ADDRESS (if different from Controlling Office)		15. SECURITY CLASS. (of this report) unclassified	
		15a. DECLASSIFICATION/DOWNGRADING SCHEDULE	
16. DISTRIBUTION STATEMENT (of this Report)			
17. DISTRIBUTION STATEMENT (of the abstract entered in Block 20, if different from Report)			
18. SUPPLEMENTARY NOTES			
19. KEY WORDS (Continue on reverse side if necessary and identify by block number) crack tip, moving crack, nonlocal elasticity			
20. ABSTRACT (Continue on reverse side if necessary and identify by block number) Stress distribution near the tip of a constant velocity crack is determined by means of the nonlocal theory of elasticity. The stress at the crack tip is finite and it decreases with increasing crack velocity.			

DD FORM 1 JAN 73 1473 EDITION OF 1 NOV 65 IS OBSOLETE

SECURITY CLASSIFICATION OF THIS PAGE (When Data Entered)



FINAL REPORT

MOVING NONLOCAL CRACK: ANTI-PLANE SHEAR CASE

N. Ari⁺ and A.C. Eringen

Princeton University
Princeton, NJ 08544

ABSTRACT: Stress distribution near the tip of a constant velocity crack is determined by means of the nonlocal theory of elasticity. The stress at the crack tip is finite and it increases with increasing crack velocity.

I. INTRODUCTION

The present work is concerned with the investigation of the stress distribution near the tip of a uniformly moving crack in a brittle elastic solid. To this end, we employ the recently developed theory of nonlocal elasticity [1] which incorporates important features of atomic lattice dynamics relevant to the study of microscopic defects, as well as macroscopic phenomena that fall within the domain of classical elasticity in the long wave-length limit.

*Supported by the Office of Naval Research.

⁺Present address: Research Institute for Basic Sciences, Applied Mathematics Department, P.O. Box 74, Gebze, Turkey.

LIBRARY
RESEARCH REPORTS DIVISION
NAVAL POSTGRADUATE SCHOOL
MONTEREY, CALIFORNIA 93943



RESEARCH IN MICROMECHANICS

FINAL REPORT

"MOVING NONLOCAL CRACK: ANTI-PLANE SHEAR CASE"

N. Ari and A.C. Eringen

Task No. NR 064-410
N00014-76-C-0240 Mod 4

OFFICE OF NAVAL RESEARCH

84-SM-13

DEPARTMENT OF CIVIL ENGINEERING
SCHOOL OF ENGINEERING/APPLIED SCIENCE
PRINCETON UNIVERSITY,
PRINCETON, NEW JERSEY 08544

December 1984

In a series of papers, Eringen and his coworkers [2-6] treated various problems on crack tip stresses, dislocations and dispersive wave propagation by means of the linear theory of nonlocal elasticity. We mention here briefly, the following few basic results in support of the power and the potential of nonlocal theory: In contrast to the predictions made in classical elasticity:

- (i) Plane waves are dispersive and the dispersion curves approximate those of the atomic lattice dynamics and the phonon-dispersion experiments within a 6% error margin in the entire Brillouin zone [1-3].
- (ii) The hoop stress is finite and acquires a maximum near the crack tip. Consequently, physically meaningful maximum stress hypothesis may be used at all levels as a fracture criterion [4-8].
- (iii) Theoretical strength of solids estimated by means of nonlocal theory is in excellent agreement with the predictions based on atomic theory [9,10].

In dynamic problems of crack propagation, classical theory also predicts infinite stresses at the crack tip. Moreover, the critical dynamic stress intensity factors (i.e. $K = r^{1/2}(t_{yy}, t_{yz})$ as $r \rightarrow 0$ and $\theta = 0$) turn out to be independent of the crack velocity, identical to their static values [11,12].

The problem of a constant velocity crack offers a convenient testing ground for the extension of the treatment of nonlocal crack problems to dynamic cases. Here, we study the motion of a finite length crack for the anti-plane shear case (Mode III). This problem represents an oversimplified picture of the dynamic fracture. Nevertheless, it does offer us an

insight on the nature of the nonlocal stress field near the tip of a moving crack. It is found that the nonlocal shear stress at the crack tip is finite and it increases with increasing crack velocity. These characteristics of nonlocal stress behavior enables us to extend the maximum stress hypothesis to the dynamic cases.

In Section 2, we summarize basic equations of nonlocal elasticity. In Section 3, an analytical (approximate) solution is obtained for the dual integral equations ensuing from the mixed boundary value problem. The nonlocal stress field is given in Section 4, and compared with the local and the static stresses.

II. NONLOCAL ELASTICITY

For linear homogeneous and isotropic elastic solids, the two dimensional stress constitutive equations are given by [1]:

$$t_{k\ell} = \int_S \alpha(|\underline{x}' - \underline{x}|, \epsilon) \sigma_{k\ell}(\underline{x}') ds(\underline{x}') \quad (2.1)$$

where S is the two-dimensional plane region and $\sigma_{k\ell}(\underline{x}', t)$ is the local (classical) stress tensor at \underline{x}' which depends only on the local strain tensor $e_{k\ell}(\underline{x}', t)$ at the point \underline{x}' , where

$$\sigma_{k\ell} = \lambda e_{rr} \delta_{k\ell} + 2\mu e_{k\ell} \quad (2.2)$$

$$e_{k\ell} = \frac{1}{2} (u_{k,\ell} + u_{\ell,k}) \quad (2.3)$$

Here u_k is the displacement vector, λ and μ are the Lamé constants, and an index following a comma represents a gradient, e.g.

$$u_{k,\ell} = \frac{\partial u_k}{\partial x_\ell}$$

The nonlocal kernel $\alpha(|\tilde{x}' - \tilde{x}|, \epsilon)$ characterizes the range and the strength of interatomic interactions. ϵ is the nonlocality parameter. It corresponds to an internal characteristic length of the material, hence reflects the microstructure and discreteness of the body. The nonlocal kernels may be determined by requiring that the wave dispersion equations derived from the nonlocal equations approximate the corresponding dispersion relations which are derived by means of lattice dynamics or obtained experimentally. In addition, they must fulfill certain consistency conditions so that in the case $\epsilon \rightarrow 0$ (the continuum limit), the nonlocal equations revert to the classical, local equations, i.e.

$$\begin{aligned} \text{(i)} \quad \lim_{\epsilon \rightarrow 0} \alpha(|\tilde{x}' - \tilde{x}|, \epsilon) &= \delta(\tilde{x}' - \tilde{x})^* \\ \text{(ii)} \quad \int_S \alpha(|\tilde{x}' - \tilde{x}|) dS(\tilde{x}') &= 1 \\ \text{(iii)} \quad \alpha \text{ vanishes as } |\tilde{x}' - \tilde{x}| &\rightarrow \infty \end{aligned} \quad (2.4)$$

In [5], we introduced a two-dimensional kernel which satisfies the consistency conditions and also yields dispersion curves closely approximating those of a two-dimensional perfect square lattice. (For other possibilities, see [3,9])

$$\alpha(|\tilde{x}' - \tilde{x}|, \epsilon) = (2\pi \epsilon^2)^{-1} K_0(\epsilon^{-1} [(x' - x)^2 + (y' - y)^2]^{\frac{1}{2}}) \quad (2.5)$$

* We note that the homogeneous kernel $\alpha(|\tilde{x}' - \tilde{x}|)$ used here violates the inhomogeneity that exists in an atomically thin layer near the crack boundary.

(2.5) has the additional convenient property that

$$(1 - \epsilon^2 \nabla^2) \alpha = \delta(|\underline{x}' - \underline{x}|) \quad (2.6)$$

For perfect crystals, the dispersion curve can be matched exactly at the ends of the Brillouin zone, leading to the determination of ϵ :

$$\epsilon = (0.22 - 0.31) a \quad (2.7)$$

where a is the atomic lattice parameter.

In the sequel, we will use (2.5) as the nonlocal kernel and ϵ as given by (2.7) so that there will be no parameter adjustments for the specific problem treated here.

Cauchy's equations for the linear momentum remains valid:

$$t_{k\ell,k} = \rho \ddot{u}_\ell \quad (2.8)$$

where ρ is the mass density and a superposed dot denotes the material time derivative.

Upon applying the operator (2.6) to (2.1) and using (2.3) and (2.4), we obtain the following singularly perturbed partial differential equations:

$$(1 - \epsilon^2 \nabla^2) \rho \ddot{u}_\ell = (\lambda + \mu) u_{k,k\ell} + \mu u_{\ell,kk} \quad (2.9)$$

In Section 3, we obtain the solution of Eqs. (2.9) and (2.1) for the nonlocal moving shear crack problem.

III. ANTI-PLANE MOVING CRACK

A line crack of length 2ℓ is assumed to propagate with a constant velocity V , in an elastic plate in the $X_3 = 0$ -plane. The uniform motion of the crack is maintained by an anti-plane shear stress τ_0 (Fig. 1). In the moving coordinate system

$$x = X - Vt \quad y = Y \quad (3.1)$$

we have

$$u_1 = 0, \quad u_2 = 0, \quad u_3 = w(x, y) = w(-x, y) \quad (3.2)$$

$$\sigma_{xz} = \mu \frac{\partial w}{\partial x} \quad \sigma_{yz} = \mu \frac{\partial w}{\partial y} \quad (3.2)$$

and the field equations (2.9) reduce to

$$(V/c_2)^2 \left[1 - \varepsilon^2 \left(\frac{\partial^2}{\partial x^2} + \frac{\partial^2}{\partial y^2} \right) \right] \frac{\partial^2 w}{\partial x^2} = \left(\frac{\partial^2}{\partial x^2} + \frac{\partial^2}{\partial y^2} \right) w \quad (3.3)$$

where $c_2 = (\mu/\rho)$ denotes the phase velocity of shear waves.

We note that the nonlocal field equations revert to the local equations for $\varepsilon = 0$ and to the static equations for $V = 0$.

By utilizing the Fourier transform in the x -direction

$$\bar{f}(k, y) = (2\pi)^{\frac{1}{2}} \int_{-\infty}^{\infty} f(x, y) \exp(ikx) dk \quad (3.4)$$

we obtain the general solution of (3.3) for $y \geq 0$ as

$$\bar{w}(k, y) = \left(\frac{2}{\pi}\right)^{\frac{1}{2}} \int_0^{\infty} A(k) \exp(-k \gamma(\epsilon k) y - i k x) dk \quad (3.5)$$

where

$$\gamma^2 = (c_2^2 - v^2 - \epsilon^2 v^2 k^2) / (c_2^2 - \epsilon^2 v^2 k^2) \quad (3.6)$$

and the inversion contour is chosen in such a way that

$$\Re \gamma \geq 0$$

The boundary conditions for the moving crack problem in the new coordinate system are equivalent to the static case. Here we follow [5] in determining the self-consistent nonlocal boundary conditions.* For the uniform shear load τ_0 , they are given by

$$\begin{aligned} w(x, 0) &= 0 & |x| > \ell \\ \sigma_{yz}(x, 0) &= -\tau_0, & |x| < \ell \\ w(x, y) &= 0 & \text{as } (x^2 + y^2) \rightarrow \infty \end{aligned} \quad (3.7)$$

Insertion of (3.5) into (3.2) and (3.7) yields a set of dual integral equations

$$\begin{aligned} \int_0^{\infty} \kappa D(\kappa) \gamma(\epsilon \kappa) \cos \kappa \xi \, d\kappa &= 1; & |\xi| < 1 \\ \int_0^{\infty} D(\kappa) \cos \kappa \xi \, d\kappa &= 0; & |\xi| > 1 \end{aligned} \quad (3.8)$$

where

* The use of a different set of boundary conditions are explored in other work (e.g. [10]).

$$\xi = x/\ell, \quad \kappa = k\ell \quad \delta = \varepsilon/\ell$$

$$D(\kappa) = \left(\frac{2}{\pi}\right)^{1/2} (\mu_0/\tau_0 \ell^2) A(k) \quad (3.9)$$

The standard Ansatz

$$D(\kappa) = \int_0^1 t^{1/2} h(t) J_0(\kappa t) dt \quad (3.10)$$

leads to a single Fredholm equation

$$h(t) + \int_0^1 K(t, \eta) h(\eta) d\eta = t^{1/2}; \quad 0 < t < 1 \quad (3.11)$$

where

$$K(t, \eta) = (t\eta)^{1/2} \int_0^\infty \kappa [Q(\kappa) - 1] J_0(\kappa t) J_0(\kappa \eta) d\kappa \quad (3.12)$$

$$Q(\kappa) = [(c^2 - \kappa^2)/(d^2 - \kappa^2)]^{1/2} \quad ; \quad \kappa \notin (c, d)$$

$$= i [(\kappa^2 - c^2)/(d^2 - \kappa^2)]^{1/2} \quad ; \quad \kappa \in (c, d)$$

$$d = c_2/\delta V, \quad c^2 = d^2 - 1/\delta^2 \quad (3.13)$$

The kernel $K(t, \eta)$ can be expressed in a more compact form by reducing (3.13) to an integral around the branch cuts by contour integration (see also [9], p. 286), i.e.

$$K(t, \eta) = (t\eta)^{1/2} \int_C^d \kappa Q(\kappa) \left\{ \begin{array}{l} H_0^{(1)}(\kappa t) J_0(\kappa \eta) \\ H_0^{(1)}(\kappa \eta) J_0(\kappa t) \end{array} \right\} d\kappa \quad \begin{array}{l} ; \quad t > \eta \\ ; \quad t < \eta \end{array} \quad (3.15)$$

where $H_V^{(j)}$ denote Hankel functions.

In order to derive (3.14), we first evaluate the auxiliary integrals

($t > \eta$)

$$I_j = (t\eta)^{\frac{1}{2}} \int_{C_j} z [G(z) - 1] H_0^{(j)}(zt) J_0(z\eta) dz ; \quad j=1,2 \quad (3.15)$$

$$G(z) = \begin{cases} Q(z) & ; \quad z \in C_1 \\ \bar{Q}(z) & ; \quad z \in C_2 \end{cases}$$

where a bar denotes the complex conjugate and $z = p + iq$ is a point in the complex plane. The contours C_1 and C_2 are shown in Fig. 2. There are no singularities within these contours ($I_1 = 0, I_2 = 0$) and contributions from the circular arcs vanish, due to the asymptotic behavior of the integrands on each C_j . As the next step, we recall that

$$H_0^{(1)}(z) \pm H_0^{(2)}(z) = 2 \begin{cases} J_0(z) \\ i Y_0(z) \end{cases} \quad (3.16)$$

$$H_0^{(1)}(iqt) J_0(iq\eta) = -H_0^{(2)}(-iqt) J_0(-iq\eta)$$

and we obtain

$$\begin{aligned} I_1 + I_2 &= K(t, \eta) - (t\eta)^{1/2} \int_c^d Q(\kappa) J_0(\kappa t) J_0(\kappa \eta) d\kappa \\ &\quad - (t\eta)^{1/2} \int_c^d Q(\kappa) i Y_0(\kappa t) J_0(\kappa \eta) d\kappa = 0 \end{aligned} \quad (3.17)$$

(3.14) follows easily from (3.17). For $\eta > t$, we merely exchange the roles of η and t and recover (3.14).

The new form of $K(t, \eta)$ activates us for the trial solution

$$h(t) = t^{1/2} \left[\beta + \int_c^d p(s) J_0(st) ds \right] \quad (3.18)$$

Substituting (3.18) into (3.11), we obtain

$$\begin{aligned} A\beta t^{1/2} + t^{1/2} \int_c^d B(s) p(s) J_0(st) + \beta t^{1/2} \int_c^d Q(\kappa) H_1^{(1)}(\kappa) J_0(\kappa t) d\kappa \\ + t^{1/2} \int_c^d d\kappa \kappa Q(\kappa) J_0(\kappa t) \int_c^d p(s) G(\kappa, s) d\kappa = t^{1/2} \end{aligned} \quad (3.19)$$

$$A = 1 - \frac{2}{\pi} \int_c^d \left(\frac{\kappa^2 - c^2}{d^2 - \kappa^2} \right)^{1/2} \frac{d\kappa}{\kappa} = \frac{c}{d} = \left(1 - \frac{v^2}{c_2^2} \right)^{1/2} = s_2 \quad (3.20)$$

$$B(s) = 1 - \frac{2}{\pi} \int_c^d \left(\frac{\kappa^2 - c^2}{d^2 - \kappa^2} \right)^{\frac{1}{2}} \frac{\kappa d\kappa}{\kappa^2 - s^2} = 0 ; \quad c < s < d \quad (3.21)$$

$$G(\kappa, s) = [\kappa H_1^{(1)}(\kappa) J_0(s) - s J_1(s) H_0^{(1)}(\kappa)] / (\kappa^2 - s^2) \quad (3.22)$$

We set $A\beta = 1$ and $p(d) = 0$ as an integrability condition and utilize the asymptotic expansions of the Bessel function to reduce (3.19) into a simpler form for an approximate solution:

$$\begin{aligned}
& t^{1/2} \int_c^d \beta \left(\frac{2}{\pi \kappa} \right)^{1/2} \exp(i(\kappa - 3\pi/4)) Q(\kappa) J_0(\kappa t) d\kappa \\
& - t^{1/2} \int_c^d \left[\int_c^d \frac{i \exp(i(\kappa-s))}{\pi (\kappa s)^{1/2} (\kappa-s)} p(s) ds \right] \kappa Q(\kappa) J_0(\kappa t) d\kappa \\
& + t^{1/2} \int_c^d R(\kappa) Q(\kappa) J_0(\kappa t) d\kappa = 0
\end{aligned} \tag{3.23}$$

where $R(\kappa)$ is given by

$$\begin{aligned}
R(\kappa) = \kappa \int_c^d & \left[G(\kappa, s) + \frac{i \exp(i(\kappa-s))}{\pi (\kappa s)^{1/2} (\kappa-s)} \right] p(s) ds \\
& + \beta [H_1(\kappa) - \left(\frac{2}{\pi \kappa} \right)^{1/2} \exp(i(\kappa - 3\pi/4))] \tag{3.24}
\end{aligned}$$

By ignoring the last term in (3.23), we obtain an airfoil equation

$$\frac{i}{\pi} \int_c^d \frac{p(s) \exp(-is) s^{-1/2}}{\kappa - s} ds = \frac{\beta (2/\pi)^{1/2} \exp(-i3\pi/4)}{\kappa} \tag{3.25}$$

The solution of (3.25) with the side condition $p(d) = 0$ is (Tricomi [14], p. 178)

$$p(s) = -i \beta \left(\frac{c}{d} \right)^{1/2} \left(\frac{2}{\pi s} \right)^{1/2} \exp(i(s - 3\pi/4)) \left(\frac{d-s}{s-c} \right)^{1/2} \tag{3.26}$$

Substitution of (3.26) into the third term in (3.24) yields

$$\int_c^d R(\kappa) Q(\kappa) J_0(\kappa t) = r(t) = o(\epsilon^{1/2}) \quad (3.27)$$

Hence, $p(s)$ constitutes a very good approximate solution for (3.11) to the order of $(\delta^{1/2})^*$.

In the next section, we utilize the approximation provided by (3.18) and calculate the nonlocal crack tip stresses.

IV. STRESS FIELD

The nonlocal stress field can be calculated by substituting (3.18) into (3.10) and (2.1). Below, for comparison purposes, we also give the crack tip stresses for the local and the static cases. The stresses along the crack line near the crack tip ($y=0$, $\xi > 1$), are given by:

1. The Static Case: $V = 0$

The local and nonlocal field equations coincide. For both cases, the solution is given by

$$D(\kappa) = J_1(\kappa)/\kappa \quad (4.1)$$

(i) Local: $\delta = 0$

$$\begin{aligned} t_{yz}^{LS}/\tau_0 &= \int_0^\infty J_1(\kappa) \cos \kappa \xi \, d\kappa = \int_0^\infty I_1(\kappa) e^{-\kappa \xi} \, d\kappa \\ &= (\xi^2 - 1)^{-1/2} [\xi + (\xi^2 - 1)^{1/2}]^{-1}; \quad \xi > 1 \end{aligned} \quad (4.2)$$

* The approximate solution (3.26) is not as good when V becomes very close to c_2 (i.e. $c \rightarrow 0$), since then the asymptotic expansions of the Bessel functions in (3.23) are no longer valid.

The second integral in (4.2) is obtained by contour integration (i.e., $J_1(\kappa) e^{i\kappa\xi}$ on C_1 and $J_1(\kappa) e^{-i\kappa\xi}$ on C_2 (see Fig. 2)). The local stress is unbounded at the crack tip, $\xi = 1$.

(ii) Nonlocal: $\delta \neq 0$

$$t_{yz}^{NS}/\tau_0 = \int_0^\infty (1 + \delta^2 \kappa^2)^{-\frac{1}{2}} [(1 + \delta^2 \kappa^2)^{\frac{1}{2}} + \delta \kappa]^{-1} J_1(\kappa) \cos \kappa \xi \, d\kappa \quad (4.3)$$

$$= \int_0^{\delta^{-1}} I_1(\kappa) e^{-\kappa \xi} \, d\kappa + \int_{\delta^{-1}}^\infty [1 - \delta \kappa / (\delta^2 \kappa^2 - 1)^{\frac{1}{2}}] I_1(\kappa) e^{-\kappa \xi} \, d\kappa \quad (4.4)$$

$$= [2(\xi-1)]^{-\frac{1}{2}} \left[[2/(\xi+1)]^{\frac{1}{2}} [\xi + (\xi^2 - 1)^{\frac{1}{2}}]^{-1} - 1 \right] + \frac{\varepsilon^{-\frac{1}{2}}}{2} \chi^{\frac{1}{2}} [K_{3/4}(\chi) I_{1/4}(\chi) + K_{1/4}(\chi) I_{3/4}(\chi)] + O(1)$$

$$\chi = (\xi-1)/2\delta \quad (4.5)$$

From (4.5) and from the small argument behavior of the Bessel functions, we observe that the crack tip stress is finite

$$t_{yz}^{NS}(1,0)/\tau_0 = \sqrt{2}(\Gamma(3/4)/\Gamma(1/4))\delta^{\frac{1}{2}} = 0.475 \delta^{\frac{1}{2}} \quad (4.6)$$

The difference between (4.3) and (4.2) lies in the terms which include the nonlocality parameter $\delta = \varepsilon/\ell$. They act as a converging factor in (4.3) and the nonlocal stress is bounded. Equation (4.4) is obtained by contour integration methods, using the contours C_1 and C_2 (Fig. 2). Here we see how the nonlocality acts as a natural cut-off in the Fourier domain and thus bringing in the discreteness effects of a nonlocal body.

2. The Dynamic Case: $V \neq 0$

(i) Local: $\delta = 0$

The solution for $D(\kappa)$ is different from the static case

$$D(\kappa) = \frac{J_1(\kappa)}{\kappa} \left(1 - \frac{V^2}{c_2^2}\right)^{-1/2} = J_1(\kappa) / (s_2 \kappa) \quad (4.7)$$

Nevertheless, the local stress is equal to its static value and it is unbounded

$$t_{yz}^{LD} / \tau_0 = \int_0^\infty s_2 \kappa D(\kappa) \cos \kappa \xi \, d\kappa = \int_0^\infty J_1(\kappa) \cos \kappa \xi \, d\kappa \quad (4.8)$$

(ii) Nonlocal: $\delta \neq 0$

$$\begin{aligned} t_{yz}^{ND} / \tau_0 &= \beta \int_0^\infty (1 + \delta^2 \kappa^2)^{-\frac{1}{2}} [(1 + \delta^2 \kappa^2)^{\frac{1}{2}} + \delta \kappa Q(\kappa)]^{-1} \kappa Q(\kappa) D(\kappa) \cos \kappa \xi \, d\kappa \\ &= \int_0^{\delta^{-1}} B(\kappa) I_1(\kappa) e^{-\kappa \xi} \, d\kappa \\ &+ \int_{\delta^{-1}}^\infty (1 - \delta \kappa [(c_2^2 - V^2 - \delta^2 V^2 \kappa^2) / (c_2^2 - \delta^2 V^2 \kappa^2) (\delta^2 \kappa^2 - 1)]^{\frac{1}{2}}) B(\kappa) I_1(\kappa) e^{-\kappa \xi} \, d\kappa \\ &+ o(1); \end{aligned}$$

where

$$B(\kappa) = \frac{1}{2} (1 - V^2 / c_2^2)^{-1/4} \left[\left(\frac{d + i\kappa}{c + i\kappa} \right)^{\frac{1}{2}} + \left(\frac{d - i\kappa}{c - i\kappa} \right)^{\frac{1}{2}} \right]$$

In Fig. 3, the numerical evaluation of (4.9) are plotted along with the local anti-plane shear stress. In contrast to the local stress, the non-local stress is increasing with the increasing crack velocity.

In this work, we have focused on how the nonlocality affects the stress distribution. In an upcoming publication, we will discuss the implications of the velocity dependence of the nonlocal crack tip stresses for brittle crack propagation. The extension of the maximum stress hypothesis to the dynamic case and the determination of a terminal velocity will be discussed in the context of a constant velocity crack in in-plane extension mode, which provides a more realistic picture of dynamic rupture phenomena.

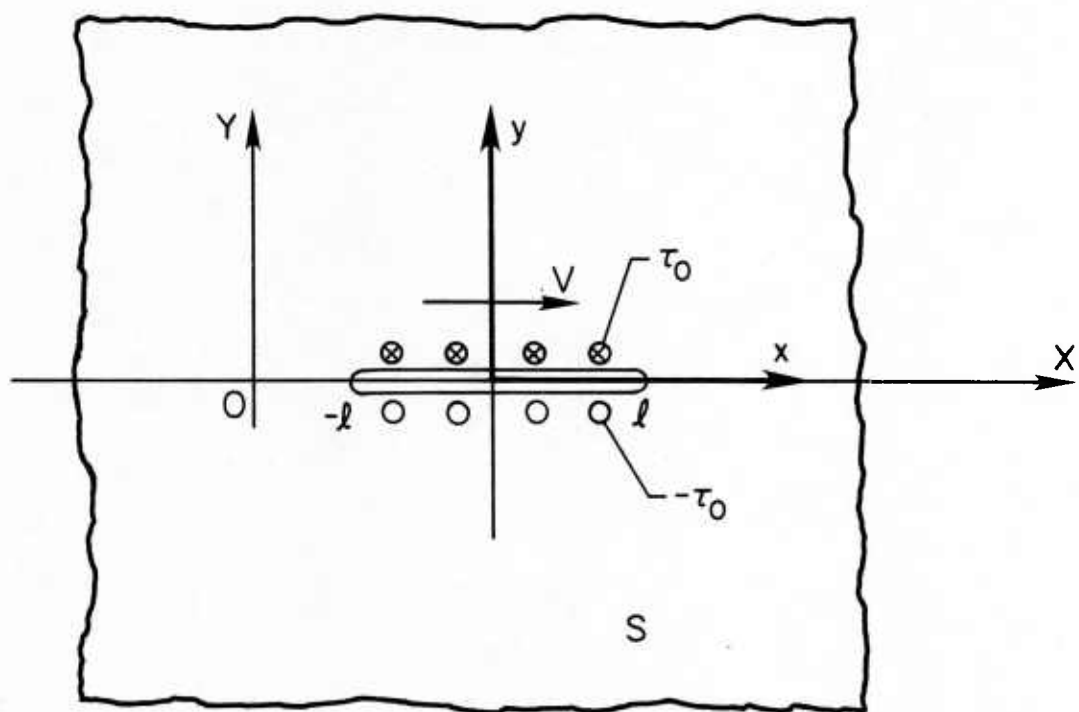


FIGURE 1
MOVING ANTI-PLANE CRACK

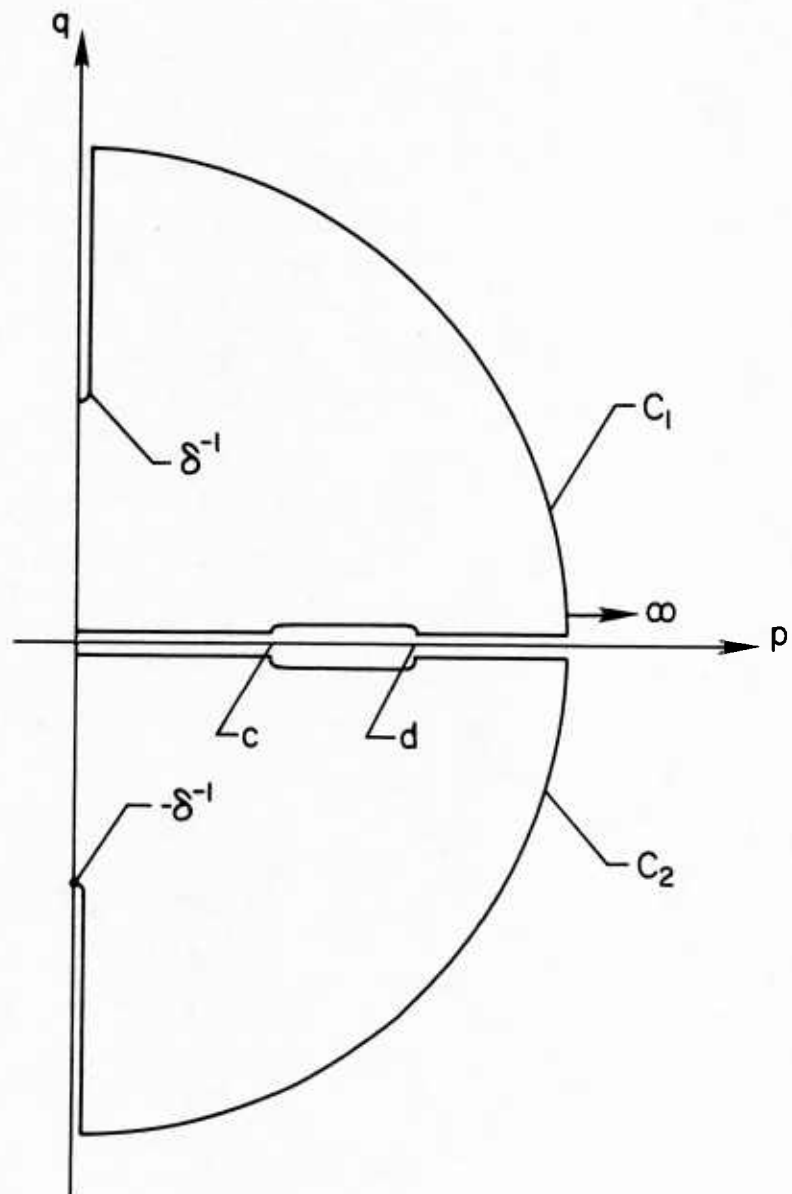


FIGURE 2
CONTOURS IN THE COMPLEX PLANE

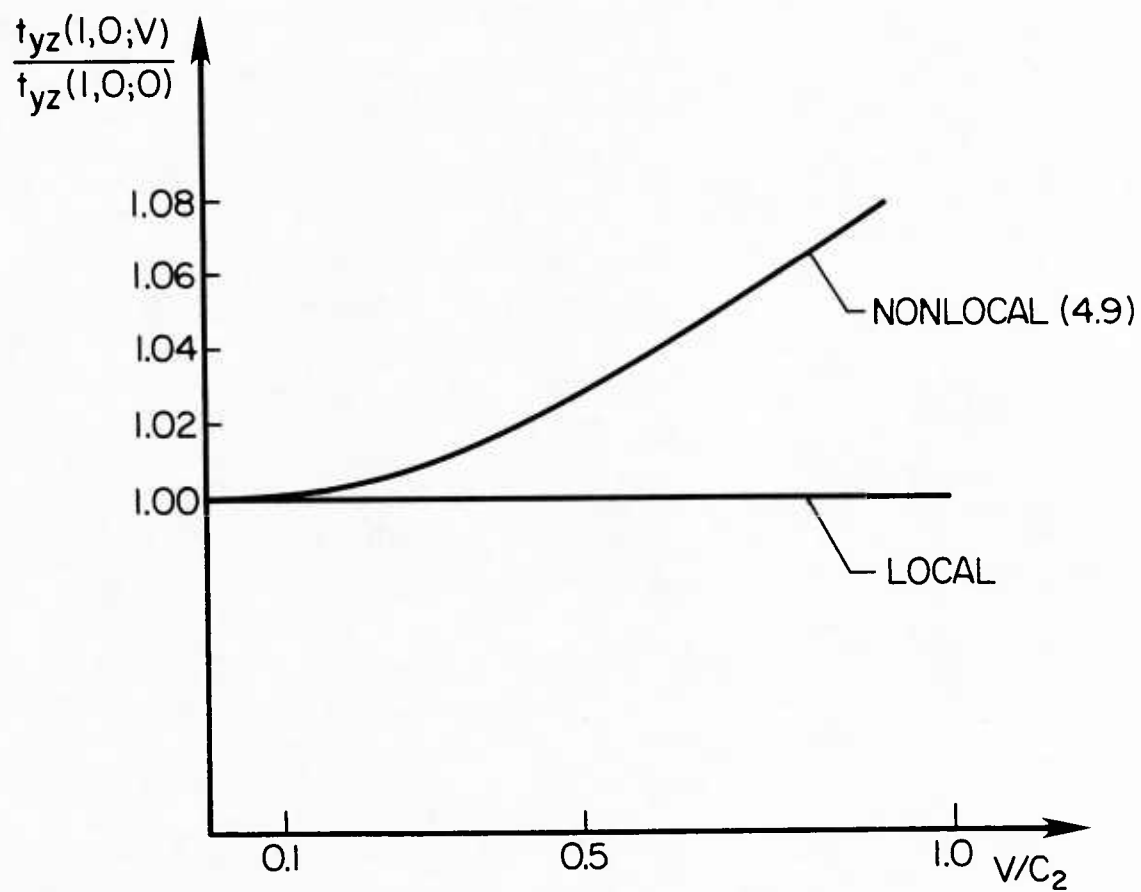


FIGURE 3
THE NONLOCAL STRESS

REFERENCES

- [1] Eringen, A.C., Int. J. Engng. Sci., 10, 425 (1972), see also Continuum Physics, Vol. IV, edited by A.C. Eringen, Academic Press, 1976, pp.
- [2] Eringen, A.C., "Nonlocal Continuum Mechanics and Some Applications," in Nonlinear Equations in Physics and Mathematics, edited by A.O. Barut, Reidel Publishing Company, 271, 1977.
- [3] Eringen, A.C., J. Applied Physics, 59, 4703, 1983.
- [4] Eringen, A.C., C.G. Speziale and B.S. Kim, J. Mech. Phys. Solids, 25, 339 (1977).
- [5] Ari, N. and A.C. Eringen, Cryst. Latt. Def. and Amorph. Mat., 10, 33 (1983).
- [6] Eringen, A.C., Engineering Fracture Mechanics, 12, 211 (1979).
- [7] Eringen, A.C., J. Phys. D: Appl. Phys., 10, 671 (1977).
- [8] Eringen, A.C., Int. J. Engng. Sci., 15, 177 (1977).
- [9] Eringen, A.C., Crystal Lattice Defects, 7, 109, 1977.
- [10] Eringen, A.C., J. Applied Physics, 54, 6811, 1983.
- [11] Yoffe, E.H., Phil. Mag., 42, 739 (1951).
- [12] Sih, G.C. and Y. M. Chen, in Elastodynamic Crack Problems, Ed. by G.C. Sih, p. 74, Int. Pub. Co., Noordhoff (1977).
- [13] Kanwal, R.P., Linear Integral Equations, Academic Press, New York (1971).
- [14] Tricomi, F.G., Integral Equations, Interscience Publishers, New York (1957).

DISTRIBUTION LIST-SOLID MECHANICS

Office of Naval Research
800 N. Quincy Street
Arlington, VA 22217
Attn: Code 432 (4 copies)

Defense Documentation Center (12 copies)
Cameron Station
Alexandria, VA 22314

Naval Research Laboratory
Washington, DC 20375
Attn: Code 6370
Code 6380
Code 5830
Code 6390
Code 2620

David W. Taylor Naval Ship Research
and Development Center
Bethesda, MD 20084
Attn: Code 1700
Code 1720
Code 1720.4
Code 1844

Naval Air Development Center
Warminster, PA 18974
Attn: Code 6043
Code 6063

Naval Surface Weapons Center
White Oak, MD 20910
Attn: Code K20
Code R13
Technical Library

Naval Surface Weapons Center
Dahlgren, VA 22448
Attn: Technical Library

Naval Underwater Systems Center
New London, CT 06320
Attn: Code 44
Technical Library

Naval Underwater Systems Center
Newport, RI 02841
Attn: Technical Library

Naval Weapons Center
China Lake, CA 93555
Attn: Technical Library

Chief of Naval Operations
Department of the Navy
Washington, DC 20350
Attn: Code OP-098

Commander
Naval Sea Systems Command
Washington, D.C. 20362
Attn: Code 05R25
Code 05R26
Code 55Y
Code 55Y2

Commander
Naval Air Systems Command
Washington, DC 20361
Attn: Code 03D
Code 7226
Code 310A
Code 310B

U. S. Naval Academy
Mechanical Engineering Department
Annapolis, MD 21402

Naval Postgraduate School
Monterey, CA 93940
Attn: Technical Library

Mr. Jerome Persh
Staff Specialist for Materials and Structures
OUSDRE&E, The Pentagon
Room 3D1089
Washington, DC 20301

Dr. Clifford Astill
Solid Mechanics Program
National Science Foundation
Washington, D.C. 20550

Major David Glasgow
Aerospace Sciences Directorate
Air Force Office of Scientific Research
Bolling Air Force Base
Washington, DC 20332

Dr. A. Amos
Aerospace Sciences Directorate
Air Force Office of Scientific Research
Bolling Air Force Base
Washington, DC 20332

Dr. E. Saibel
Engineering Sciences Division
P.O. Box 12211
Research Triangle Park, NC 27709

Dr. Harold Liebowitz, Dean
School of Engineering and Applied Science
George Washington University
Washington, DC 20052

Professor L.B. Freund
Brown University
Division of Engineering
Providence, RI 02912

Professor B. Budiansky
Harvard University
Division of Applied Sciences
Cambridge, MA 02138

Professor S. N. Atluri
Georgia Institute of Technology
School of Civil Engineering and Mech.
Atlanta, GA 30332

Professor J. D. Achenbach
Northwestern University
Department of Civil Engineering
Evanston, IL 60201

Professor D. M. Parks
Massachusetts Institute of Technology
Department of Mechanical Engineering
Cambridge, MA 02139

Prof. S. S. Wang
University of Illinois
Dept. of Theoretical & Applied Mechanics
Urbana, IL 61801

Prof. Y. Weitsman
Texas A&M University
Civil Engineering Department
College Station, TX 77843

Prof. I. M. Daniel
Illinois Institute of Technology
Dept. of Mechanical Engineering
Chicago, IL 60616


Prof. G. J. Dvorak
Rensselaer Polytechnic Institute
Department of Civil Engineering
Troy, New York 12181

Mr. C. R. Barnes
Battelle Columbus Laboratories
505 King Avenue
Columbus, OH 43201

Dr. R. M. Christensen
Lawrence Livermore National Laboratory
Chemistry & Material Science Department
P.O. Box 80P
Livermore, CA 94550

Prof. J.R. Rice
Harvard University
Division of Applied Sciences
Cambridge, MA 02138

~~Prof. A.C. Eringen~~
~~Princeton University~~
~~Department of Aerospace and Mechanical Sciences~~
~~Princeton, New Jersey 08540~~



Prof. P. M. Naghdi
University of California
Department of Mechanical Engineering
Berkeley, California 94720

Prof. R. A. Schapery
Texas A & M University
Department of Civil Engineering
College Station, Texas 77843

Prof. G. Herrmann
Stanford University
Department of Applied Mechanics
Stanford, California 94305

Dr. T. L. Geers
Lockheed Missiles and Space Company
3251 Hanover Street
Palo Alto, California 94303

Dr. R.S. Dunham
Anatech International Corp.
3344 North Torrey Pines Court
Suite 320
LaJolla, CA 92037

Prof. S. W. Lee
University of Maryland
Department of Aerospace Engineering
College Park, MD 20742

Dr. R. F. Jones
David W. Taylor Naval Ship R & D Center
Code 172
Bethesda, MD 20084

Prof. J. T. Oden
University of Texas at Austin
Department of Aerospace Engineering
and Engineering Mechanics
Austin, Texas 78712-1085

Prof. I. Fried
Boston University
Department of Mathematics
111 Cummington Street
Boston, MA 02215

Prof. H. Murakami
University of California, San Diego
Department of Applied Mechanics and
Engineering Sciences
LaJolla, CA 92093

Prof. J.N. Reddy
Virginia Polytechnic Institute and
State University
Department of Engineering Science and
Mechanics
Blacksburg, VA 24061

Prof. E. Becker
University of Texas
Department of Engineering Mechanics
Austin, Texas 78712-1085

Prof. P. Pinsky
Stanford University
Department of Civil Engineering
Stanford, CA 94305

Prof. T.J.R. Hughes
Stanford University
Division of Applied Mechanics
Stanford, CA 94305